On the Constrained Attitude Control Problem*

Yoonsoo Kim,[†] Mehran Mesbahi[‡]
Department of Aeronautics & Astronautics
University of Washington
Seattle, WA 98195
and
Gurkirpal Singh,[§] Fred Y. Hadaegh[¶]
Jet Propulsion Laboratory
California Institute of Technology
Pasadena, CA 91109

In this paper, we consider various classes of constrained attitude control (CAC) problem in single and multiple spacecraft settings. After categorizing attitude constraints into four distinct types, we provide an overview of the existing approaches to this problem. We then proceed to further expand on a recent algorithmic approach to the CAC problem. The paper concludes with an example demonstrating the viability of the proposed algorithm for a multiple spacecraft constrained attitude reconfiguration scenario.

---

*July 2004.
[†]Graduate Student. Email: *yoonsoo@aa.washington.edu*
[‡]Corresponding author. Assistant Professor. Email: *mesbahi@aa.washington.edu*
[§]Senior Technical Staff. Email: *gurkirpal.singh@jpl.nasa.gov*
[¶]Senior Research Scientist. Associate Fellow AIAA. Email: *fred.y.hadaegh@jpl.nasa.gov*

Nomenclature

$\mathbf{R}$	= real numbers
$\mathbf{R}^{m\times n}$	= $m \times n$ real matrices
$\mathbf{S}^n$	= $n \times n$ real symmetric matrices
$\mathbf{S}^n_+$	= $n \times n$ positive semidefinite matrices; also denoted as in $P \geq 0$
$\mathbf{S}^n_{++}$	= $n \times n$ positive definite matrices; also denoted as in $P > 0$
I_n	= $n \times n$ identity matrix
$0_{m\times n}$	= $m \times n$ zero matrix
J_i	= rigid body inertia along principle axis i ($i = 1, 2, 3$)
A, J, Q, R, Ω	= constant real matrices
q	= unit quaternion; $q = [q_1,\ q_2,\ q_3,\ q_4]^T := [q_o^T,\ q_4]^T$
v_B, v	= unit vectors describing the direction of instrument's bore-sight in body and inertial coordinate frames, respectively
w_B, w	= unit vectors describing directions of a celestial object or thrust in body and inertial coordinate frames, respectively
u	= control torque
ω	= angular velocity vector
$\lVert x \rVert$	= 2-norm of vector x, i.e., $(x^T x)^{1/2}$
$\mathbf{B}_\eta$	= the set of vectors with η 2-norm
$\widehat{\mathbf{B}}_\eta$	= the set of vectors with 2-norm greater than or equal to η
$\mathbf{W}$	= feasible set defined by quadratic constraints
θ	= angle (in degrees)
$\alpha, \beta, \gamma, \eta, \kappa, \phi$	= constant real numbers
k, M, N	= nonnegative constants
V, Φ	= repulsive potential functions
f, g	= real-valued functions
$s(k_a, k_b)$	= sum of indexed terms starting with index k_a and ending with index k_b
$[t_0\ t_f]$	= maneuver time interval
Δt	= sampling interval for time discretization
SC	= spacecraft

I Introduction

The constrained attitude control (CAC) problem considered in this paper is as follows: given initial and terminal conditions on the angular velocity vector $\omega(t)$ and the attitude quaternion $q(t)$,

$$\omega(t_0),\ q(t_0), \quad \text{and} \quad \omega(t_f),\ q(t_f),$$

with

$$\omega(t) = [\omega_1(t), \omega_2(t), \omega_3(t)]^T \in \mathbf{R}^3, \quad q(t) = [q_1(t), q_2(t), q_3(t), q_4(t)]^T \in \mathbf{R}^4,$$

determine control torques $u_i(t) \in \mathbf{R}^3$ $(i = 1, 2, 3)$ over the time interval $t \in [t_0\ t_f]$ subject to:

- dynamic constraints

$$J_1\,\dot\omega_1(t) - (J_2 - J_3)\,\omega_2(t)\,\omega_3(t) = u_1(t), \tag{1}$$
$$J_2\,\dot\omega_2(t) - (J_3 - J_1)\,\omega_3(t)\,\omega_1(t) = u_2(t), \tag{2}$$
$$J_3\,\dot\omega_3(t) - (J_1 - J_2)\,\omega_1(t)\,\omega_2(t) = u_3(t), \tag{3}$$

  where J_i is the rigid body inertia along principle axis i,

- bounded angular velocities and control torques, i.e., for given constants $\gamma_1, \gamma_2 > 0$,

$$|\omega_i(t)| \le \gamma_1 \quad \text{and} \quad |u_i(t)| \le \gamma_2, \quad i = 1, 2, 3, \tag{4}$$

- norm preserving kinematic constraint

$$\dot q(t) = \frac{1}{2}\,\Omega(t)\,q(t), \tag{5}$$

  where

$$\Omega(t) = \begin{bmatrix} 0 & \omega_3(t) & -\omega_2(t) & \omega_1(t) \\ -\omega_3(t) & 0 & \omega_1(t) & \omega_2(t) \\ \omega_2(t) & -\omega_1(t) & 0 & \omega_3(t) \\ -\omega_1(t) & -\omega_2(t) & -\omega_3(t) & 0 \end{bmatrix},$$

  and $\|q(t)\| = 1$ for all $t \in [t_0\ t_f]$, and finally,

- attitude constraints represented by

$$f_i(q(t)) < \phi_0, \quad \text{for all } t \in [t_a\ t_b],\ i = 1, 2, \ldots, m, \tag{6}$$

or

$$\int_{t_a}^{t_b} g_i(q(t))\, dt < \phi_1, \quad i = 1, 2, \ldots, m, \tag{7}$$

for the proper functions f_i and g_i ($i = 1, \ldots, m$), constants ϕ_0, ϕ_1, and time interval $[t_a\ t_b] \subseteq [t_0\ t_f]$.

The CAC problem appears in almost every space science mission equipped with heat or light sensitive instruments, e.g., cryogenically cooled infrared telescopes, star trackers, and low energy ion composition analyzers. A representative set of such missions include Cassini mission to Saturn,[1] FIRST/Planck,[2] and SAMPEX (Solar, Anomalous, and Magnetospheric Particle Explorer).[3] In all such missions, on-board sensitive instruments are required to be protected from exposure to bright or heat generating objects. As a consequence, all reorientation and re-targeting maneuvers have to be realized via solving the constrained attitude control problem.

The attitude control problem in the absence of constraints (6)-(7), has of course been extensively studied in the literature; see for example Ref. 4. On the contrary, systematic approaches to the constrained version of the problem can be found in a handful of references despite its practical significance; these include Refs. 5-13. Our paper is a contribution to this latter body of research. Specifically in this work, we first review several existing results pertaining to the CAC problem. We then proceed to extend a recently proposed approach to the problem and substantiate on its wide applicability and computational efficiency.

The organization of the paper is as follows. In §II, we categorize various classes of attitude constraints that typically appear in space science missions. An overview of existing methods for solving these problems, including those relying on geometric constructions, artificial potential functions, constraint monitoring, randomized motion planning, and finally semidefinite programming, is then provided. In §III, we present an approach, based on semidefinite programming, for the general class of CAC problems. §IV concludes the paper with a representative set of simulation results that demonstrate the viability of the framework developed in §III.

II Existing Frameworks

In this section we provide an overview of the existing frameworks for solving the CAC problem. Let us first categorize the attitude constraints into four distinct types.† These include,

Type-I (static hard constraints): this class includes constraints imposed by celestial objects that are relatively stationary with respect to an inertial coordinate frame. We have in mind scenarios where there are strict non-exposure constraints on the on-board sensitive instruments with respect to celestial objects as in Refs. 1-3 and 6-10, or avoiding incoming particles around Saturn during ring-plane crossings,[1] and/or orbital debris and micro-meteoroid fluxes as in Ref. 3. In all such settings, given unit vectors v and w in the inertial coordinate frame, describing the direction of instrument's bore-sight and the bright celestial object, respectively, one requires that

$$v(t)^T w \leq \cos\theta \tag{8}$$

at each time instance, where θ is a required minimum angular separation; note that the angle between $v(t)$ and w is assumed to be in the range of $[0, \pi]$ without loss of generality.

Type-II (static soft constraints): this category includes the relaxed version of Type-I constraint above. In this case, violations of the inequality (8) are allowed, however, only for a limited time interval. For instance, the cryogenically cooled telescope can be exposed to an external heat source provided that the total heat exposure does not accumulate to be beyond some maximally allowed level.[13] Such constraints can be written in an integral form as

$$\int_{t_0}^{t_f} |v(t)^T w| \, dt \leq \phi_1,$$

where ϕ_1 is a fixed constant and the angle between $v(t)$ and w is assumed to be in the range of $[0, \pi]$.

Type-III (dynamic constraints): these constraints have not explicitly been considered in past but they are of great importance in the context of multiple spacecraft formation flying. Type-III constraints encompass scenarios where the plume generated by firing a particular thruster on one spacecraft results in damaging the sensitive instruments mounted on another spacecraft. Note that in this case, the source of attitude constraints are themselves dynamic; in fact, they can be represented by the inequality

$$v(t)^T w(t) \leq \cos\theta,$$

†As identified by the authors after an extensive literature search.

with the standing assumption that the angle between the two vectors remain in the range of $[0, \pi]$.

Type-IV (mixed constraints): in this last category, we include various possible combinations of the preceding three types of constraints. Most space science missions, particularly those involving multiple spacecraft formation flying, have mixed attitude constraints. Evidently, the presence of mixed constraints further complicates the required attitude maneuver planning and trajectory design for these missions.

II-A Geometric Algorithms

The geometric approach, as exemplified in Refs. $6-7$, relies on geometric relations between vectors v and w in (8) to handle constraints of Types I or II. The main ingredient of this framework is determining a feasible attitude trajectory prior to initiating the reconfiguration, if possible, or finding feasible attitudes whenever an avoidance maneuver is needed during the course of the attitude slew (see Refs. 3 and 13). Generally in this venue an optimal or an easily implementable on-board control for the unconstrained attitude maneuver between two arbitrary orientations is first considered. Then, the algorithm seeks an intermediate attitude $q(t_i)$ (a way-point) between $q(t_0)$ and $q(t_f)$, such that the aforementioned control strategy- without any constraint violation- can be applied for each time interval $[t_0\ t_i]$ and $[t_i\ t_f]$. A typical example for such an approach- as found in Ref. 6- involves finding a tangential exclusion path,

$$q(t_0) \rightsquigarrow q(t_i) \rightsquigarrow q(t_f),$$

such that the unconstrained maneuver planning for each subdivision can easily be accomplished (Fig. 1). Another explicit way to determine feasible intermediate attitudes for Type-I constraints is provided in Ref. 7. We note that although the geometric approach enjoys a certain level of conceptual simplicity, it is mainly applicable to problems where only a small number of constraints are present and selection of the attitude way-points is relatively straightforward.

II-B Potential Function-based Algorithms

Potential functions have been recognized as one of the main tools for handling kinematic constraints that arise not only in the CAC problem, but more generally, in a wide array of problems in robotics and related fields. The starting point for this approach as it pertains to the CAC problem, is constructing one or multiple outward vectors with respect to the constraints. Subsequently, one proceeds to linearly combine these vectors with appropriate weights to generate a "repellent" control torque with respect to the constrained set. For example in Ref. 8, the repulsive potential $V_{\alpha,\beta}$ is first defined by

$$V_{\alpha,\beta}(\theta) = \sum_{j=1}^{m} \Phi_j(\theta), \tag{9}$$

where

$$\Phi(\theta) = \alpha\, e^{-\beta \sum_{i=1}^{3}(\theta_i - \hat{\theta}_i)^2},$$

with

$$\dot{\theta}_i(t) = \sum_{j=1}^{3} \begin{bmatrix} 1 & \sin\theta_1(t)\tan\theta_2(t) & \cos\theta_1(t)\tan\theta_2(t) \\ 0 & \cos\theta_1(t) & -\sin\theta_1(t) \\ 0 & \sin\theta_1(t)\sec\theta_2(t) & \cos\theta_1(t)\sec\theta_2(t), \end{bmatrix} \omega_j(t),$$

θ is the Euler angle, $\hat{\theta}$ is the attitude angle associated with Type-I constraint (8), parameters α and β shape the potential function, and m is the number of constraints. The potential $V_{\alpha,\beta}$ (9) is then combined with functions constructed for other purposes (e.g., to minimize the maneuver time); the combination of these functions is then optimized at each time instance to obtain slew maneuvers for the required attitude reconfiguration. An analogous approach for obtaining constraint avoidance forces can be found in Ref. 7. Parallel to the same line of reasoning, an interesting direction that has been pursued in the potential function framework proceeds to characterize the set Γ of forbidden attitude quaternions via two orthonormal vectors z_1 and z_2. The vectors z_1, z_2 are then utilized in defining the repulsive potential as

$$V_k(q) = \frac{k(1-q_4)}{(q^T z_1)^2 + (q^T z_2)^2}, \tag{10}$$

where k is chosen as a positive constant.[9] Now since

$$q \text{ violates the constraints if } \quad (q^T z_1)^2 + (q^T z_2)^2 = 0,$$

one expects that the repulsive control defined as

$$u_k(q) = -\frac{\partial V_k(q)}{\partial q},$$

yields the torque required for the constrained reorientation. One of the main draw backs of this approach is that convergence to the target attitude can not be generally guaranteed. This is in light of the fact that superposition of potential functions of the form (10) often leads to functionals that are nonconvex.[†] Moreover, the existence of vectors z_1 and z_2 above, nicely characterizing the constrained set, is not ensured particularly as the number of Type-I constraints increases.

II-C Constraint Monitor Algorithms

The constraint monitor approach, as its name suggests, is based on active monitoring of constraint violations via the ground station or on-board computers. As presented in Refs. 1, 10, the constraint monitor algorithms first identifies potential constraints that will be violated if corrective actions are not taken during the attitude slew; if such constraints are found, the algorithm subsequently guides the spacecraft to assume a feasible attitude from a set of allowable orientations. In this regards, the constraint monitor algorithm resembles those based on the geometric approach, however, it is characteristically more dynamic. This approach has been successfully implemented on the Cassini mission;[10] it has the advantage of being applicable to various classes of attitude constraints. In the meantime, the issue of convergence for the constraint monitor algorithm can only be addressed in a case by case scenario. Generally, one needs to resort to extensive mission simulations to demonstrate the viability of the algorithm.

II-D Randomized Algorithms

Randomized motion planning algorithms have been introduced to solve the constrained attitude problem in Refs. 11 and 12. These algorithms are based on following ingredients: (1) initialize a graph G_0 consisting of a distinct vertex v_0 representing initial states $q(t_0)$, $\omega(t_0)$, (2) at iteration $k+1$, perform a random search, starting from v_k, to determine a set of feasible vertices among the vertices of graph G_k, (3) select a feasible vertex, among those found in (2) such that a given cost functional is minimized; call this vertex v_{k+1}, (4) repeat steps (2)-(3), now initiated from v_{k+1}; replace the index k with $k+1$. Iterate until the final attitude $q(t_f)$ is achieved, (5) apply an optimal control torque for each attitude trajectory subdivision found.

[†]In Ref. 8, it is stated that the proposed approach applied to a single Type-I constraint has a guaranteed convergence behavior.

The random search approach has the advantage that it can deal with all types of trajectory constraints. However, one of its potential drawbacks is that convergence to the final attitude can be guaranteed only in a probabilistic sense: it can shown that as the number of vertices in the state graph increases, the probability of an incorrect termination exponentially decays to zero. Meanwhile, we note that the computational effort in searching for a feasible node at each time step increases dramatically as the size of the underlying graph grows.

II-E Semidefinite Programming-based Algorithms

We conclude our overview by mentioning the recently proposed semidefinite programming (SDP) approach to constrained attitude control.[5] This approach will be shortly elaborated upon, as it provides the main theme for the present paper. The SDP approach essentially exploits the nonlinearity of dynamics and kinematic constraints on one hand, and the nonconvexity of attitude constraints on the other, to propose a convexified SDP formulation of the original CAC problem. An SDP is the optimization problem involving a linear objective functional and a constrained set defined by linear matrix inequalities (LMIs).[14] An LMI on the other hand, is an inequality over matrix variables, interpreted with respect to the positive semidefinite ordering (see Nomenclature). The advantage of such an SDP formulation of the CAC problem is not only its conceptual elegance, but also efficient solvability via the available software, e.g., Ref. 15.

III SDP Approach to CAC

We first present the core idea behind the SDP approach to handle Type-I constraints before delving into more complex situations arising in single and multiple spacecraft missions.

III-A Type-I Constraints

The SDP approach is based on the observation that Type-I constraints can be written in a compact quadratic form parameterizing admissible quaternions.[1,10] First recall that during the attitude maneuver it is required to satisfy

$$v(t)^T w \leq \cos\theta, \tag{11}$$

at each time instance, where the unit inertial vectors v and w, denote, respectively, the instrument's bore-sight and the bright, relatively stationary, celestial object; θ is a minimum angular separation allowed between $v(t)$ and w during the attitude slew and assumed to be in the range of $[0, \pi]$. We now employ the coordinate transformation formula, relating inertial and body vectors via the quaternion parameterization of the attitude,[16]

$$v(t) = v_B - 2(q_o^T q_o)\, v_B + 2(q_o^T v_B)\, q_o + 2q_4\, (v_B \times q_o); \tag{12}$$

in (12) we have adopted the notation

$$q_o := [q_1, q_2, q_3]^T,$$

and v_B represents the inertial vector v in body coordinates. Combining (11) and (12), followed by some algebraic operations, leads us to the equivalent quaternion characterization of the constrained set,

$$q(t)^T \widetilde{A}\, q(t) \leq 0, \tag{13}$$

with

$$\widetilde{A} := \widetilde{A}(v_B, w, \theta) = \begin{bmatrix} A & b \\ b^T & d \end{bmatrix} \in \mathbf{R}^{4\times 4}, \tag{14}$$

and

$$\begin{aligned} A &:= v_B w^T + w v_B^T - (v_B^T w + \cos\theta)\, I_3, \\ b &:= w \times v_B, \quad d_i := v_B^T w - \cos\theta. \end{aligned}$$

Since the matrix $\widetilde{A}$ in (13) is not positive semidefinite, the set defined by inequality (13) is nonconvex in the parameter $q(t)$. In order to derive an efficient algorithm for the CAC problem, Ref. 5 proposes a convex optimization alternative to handle constraints of the form (13). In this venue, the following proposition plays a crucial role, the proof of which can be found in Ref. 5.

Proposition III.1 *Given matrices $W_i \in \mathbf{S}^n$, $b_i \in \mathbf{R}$, $i = 1, 2, \ldots, m$, and $\eta > 0$, let*

$$\mathbf{W} := \{x \in \mathbf{R}^n \mid x^T W_i x \geq b_i,\ i = 1, 2, \ldots, m\} \cap \mathbf{B}_\eta, \tag{15}$$

be nonempty, where

$$\mathbf{B}_\eta := \{x \in \mathbf{R}^n \mid \|x\| = \eta\}.$$

Then $x \in \mathbf{B}_\eta$ is feasible for $\mathbf{W}$ if and only if it satisfies the LMIs

$$\begin{bmatrix} \mu_i \eta^2 - b_i & x^T \\ x & \widetilde{W}_i \end{bmatrix} \geq 0, \quad i = 1, \ldots, m, \tag{16}$$

where

$$\widetilde{W}_i := (\mu_i I_n - W_i)^{-1}$$

and for each i, μ_i is strictly greater than the largest eigenvalue of W_i (and thus $\widetilde{W}_i, \widetilde{W}_i^{-1} \in \mathrm{S}^n_{++}$).

One of the key relations often used in the LMI literature, hiding behind the derivation of LMIs (16), is the Schur complement formula stating that when $A > 0$,

$$\begin{bmatrix} A & B \\ B^T & C \end{bmatrix} > 0$$

if and only if $C - B^T A^{-1} B > 0$; see Ref. 14. An extension of Proposition III.1, relaxing the requirement that $x \in \mathrm{B}_\eta$, leads to the following LMI sufficiency conditions.[5]

Proposition III.2 *Let*

$$\widehat{\mathrm{B}}_\eta := \{x \in \mathrm{R}^n \mid \|x\| \geq \eta\}. \tag{17}$$

Then $x \in \widehat{\mathrm{B}}_\eta$ satisfying LMIs (16) is an element of W (15).

Propositions III.1 and III.2 are utilized in the context of constrained attitude control in the following way. Since the spacecraft attitude has been parameterized in terms of quaternions, and the quaternion trajectory $q(t)$ *implicitly* evolves on the unit ball B_1, Propositions III.1 can be employed to conclude that spacecraft constrained control attitude problem, as augmented with an *arbitrary* number of nonconvex Type-I constraints, can be represented by a (convex) SDP. In particular, this observation would completely solve the constrained attitude control if one could seamlessly augment the nonlinear kinematic equations (5) to this SDP. However, as augmenting this differential nonlinear equality constraint generally destroys the convexity of the corresponding feasible set, one needs to resort to linearization of kinematic equations. Such a linearization scheme, on the other hand, introduces errors in quaternion updates and leads to the violation of the assumption that the linearized attitude trajectory evolves on the unit ball. Nevertheless, the linearization error can be shown to be norm increasing, i.e., the approximate quaternion $\hat{q}$ is implicitly an element of $\widehat{\mathrm{B}}_1$ in Eq. (17) (see Ref. 5). In this case, Proposition III.2 can be utilized to guarantee that by solving LMIs in Eq. (16), in concert with the linearized kinematic equations, the resulting attitude constraints are not violated during the maneuver, that is, $q(t) \in \mathrm{W}$ (Eq. 15) for $t \in [t_0 \; t_f]$.

One simple approach to the linearization of kinematic and dynamic equations proceeds as follows: we consider the discretization of Eqs. (1)-(3) and (5) as,

$$\dot{x}(t) \approx \frac{x(k+1) - x(k)}{\Delta t}$$

with proper sampling time Δt ($\Delta t = 0.1$ in our simulation examples of §IV). Putting it all together, the convex optimization approach to constrained attitude control with Type-I constraints assumes the following form: we iteratively solve the problem $\mathcal{Q}_I^{(k)}$:

$$\min_{x(k)} \quad \alpha \tag{18}$$

subject to

$$x(k)^T \{H^T \tilde{A}_i H\} x(k) \leq 0, \quad i = 1, 2, \ldots, m,$$

or

$$\begin{bmatrix} \mu_i & (Hx(k))^T \\ Hx(k) & (\mu_i I_{10} + \tilde{A}_i)^{-1} \end{bmatrix} \geq 0, \quad i = 1, 2, \ldots, m, \tag{19}$$

$$\begin{bmatrix} \alpha & (E(k)^{1/2} \begin{bmatrix} x(k) \\ 1 \end{bmatrix})^T \\ E(k)^{1/2} \begin{bmatrix} x(k) \\ 1 \end{bmatrix} & I_{11} \end{bmatrix} \geq 0, \tag{20}$$

$$\begin{aligned} F(k)x(k) &= y(k), & (21) \\ |G_1 x(k)| &\leq \gamma_1 \, [1\ 1\ 1]^T, & (22) \\ |G_2 x(k)| &\leq \gamma_2 \, [1\ 1\ 1]^T, & (23) \end{aligned}$$

where $E(k) \in \mathbf{S}_+^{11}$, $F(k) \in \mathbf{R}^{7\times 10}$, $G_1, G_2 \in \mathbf{R}^{10\times 10}$, and $H \in \mathbf{R}^{4\times 10}$. In Eqs. (19)-(23) we have

$$\begin{aligned} E(k) &= \begin{bmatrix} 0_{3\times 3} & 0_{3\times 3} & 0_{3\times 4} & 0_{3\times 1} \\ 0_{3\times 3} & I_3 & 0_{3\times 4} & \omega(N) \\ 0_{4\times 3} & 0_{4\times 3} & 0_{4\times 4} & 0_{4\times 1} \\ 0_{1\times 3} & \omega(N)^T & 0_{1\times 4} & \omega(N)^T \omega(N) \end{bmatrix} \\ &+ \begin{bmatrix} 0_{6\times 6} & 0_{6\times 4} & 0_{6\times 1} \\ 0_{4\times 6} & Q(N)^T Q(N) & 0_{4\times 1} \\ 0_{1\times 6} & 0_{1\times 4} & 0_{1\times 1} \end{bmatrix}, \end{aligned}$$

$$F(k)=\left[\begin{array}{c|c|c}-\Delta t\, I_3 & J & 0_{4\times 4}\\ \hline 0_{4\times 3} & R(k+1) & I_4\end{array}\right],$$

where

$$J:=\begin{bmatrix} J_1 & 0 & 0\\ 0 & J_2 & 0\\ 0 & 0 & J_3\end{bmatrix},\quad R(k):=\frac{\Delta t}{2}\begin{bmatrix}-q_4(k) & q_3(k) & -q_2(k)\\ -q_3(k) & -q_4(k) & q_1(k)\\ q_2(k) & -q_1(k) & -q_4(k)\\ q_1(k) & q_2(k) & q_3(k)\end{bmatrix},$$

$$G_1:=\begin{bmatrix} 0_{3\times 3} & I_3 & 0_{3\times 4}\end{bmatrix},\quad G_2:=\begin{bmatrix} I_3 & 0_{3\times 7}\end{bmatrix},$$

$$x(k):=\begin{bmatrix} u_1(k)\\ u_2(k)\\ u_3(k)\\ w(k+1)\\ q(k+2)\end{bmatrix},\quad y(k):=\begin{bmatrix} J_1 w_1(k)+\Delta t\,(J_2-J_3)\,\omega_2(k)\,\omega_3(k)\\ J_2 w_2(k)+\Delta t\,(J_3-J_1)\,\omega_3(k)\,\omega_1(k)\\ J_3 w_3(k)+\Delta t\,(J_1-J_2)\,\omega_1(k)\,\omega_2(k)\\ w(k)\\ q(k+1)\end{bmatrix},$$

$$H=\begin{bmatrix} 0_{4\times 6} & I_{4\times 4}\end{bmatrix},\quad Q(N):=\begin{bmatrix} q_4(N) & q_3(N) & -q_2(N) & -q_1(N)\\ -q_3(N) & q_4(N) & q_1(N) & -q_2(N)\\ q_2(N) & -q_1(N) & q_4(N) & -q_3(N)\\ q_1(N) & q_2(N) & q_3(N) & q_4(N)\end{bmatrix},$$

μ_i is chosen to be strictly greater than the largest eigenvalue of $-\widetilde{A}_i$; the matrix $\widetilde{A}_i$ is as defined in (14). In such a setup, the SDP $\mathcal{Q}_I^{(k)}$ is solved for $x(k)$, $k=0,1,\ldots,N-1$, where $(\Delta t)N$ is the time interval $[t_0\ t_f]$ as designated for the required reorientation. Under the assumption that for each k the problem $\mathcal{Q}_I^{(k)}$ is feasible, this approach offers convergence guarantee to the final attitude, as the problems $\mathcal{Q}_I^{(k)}$ are convex programs. We note that our convex representation remains valid as long as the errors introduced by linearization are negligible; otherwise, the attitude quaternion is not guaranteed to remain on the unit ball at each time step. As it was pointed out previously, in the presence of such errors, we can still invoke Proposition III.2 and enforce the attitude exclusion zone via the SDP (18)-(23). As an alternative, one can prevent the propagation of linearization errors by using actual dynamical state $x(k)$, as opposed to those calculated from $\mathcal{Q}_I^{(k)}$, as an input data for next SDP iteration $\mathcal{Q}_I^{(k+1)}$. For instance, given $\omega(k+1)$ obtained from $\mathcal{Q}_I^{(k)}$, exact *unit* quaternion $q(k+2)$ can be computed using the equation

$$q(k+2)=e^{\frac{1}{2}\Delta t\,\Omega(k+1)}q(k+1), \tag{24}$$

where

$$\Omega(k) = \begin{bmatrix} 0 & \omega_3(k) & -\omega_2(k) & \omega_1(k) \\ -\omega_3(k) & 0 & \omega_1(k) & \omega_2(k) \\ \omega_2(k) & -\omega_1(k) & 0 & \omega_3(k) \\ -\omega_1(k) & -\omega_2(k) & -\omega_3(k) & 0 \end{bmatrix}.$$

We also note that other computational techniques for accurate quaternion updates are available (see Ref. 1), which can be used in conjunction with the proposed SDP approach.

III-B Type-II Constraints

We now consider Type-II constraints of the form

$$\int_{t_a}^{t_b} v(t)^T w \, dt \le \phi_1, \tag{25}$$

or in its discretized form

$$s(k_a, k_b) := \sum_{k=k_a}^{k_b} v(k)^T w \le \phi_1, \tag{26}$$

where $[t_a \; t_b] \subseteq [t_0 \; t_f]$ is the maneuver time interval during which we allow the constraint violation $v(t)^T w > \cos\theta$. In our short discussion of this class of constraints, we we will implicitly assume that the desired minimum angular separation satisfies $\theta \in [0, \pi/2]$; however, the case of $\theta \in [\pi/2, \pi]$ can be handled in the similar manner. As the SDP approach of §III-A is inherently a step-by-step algorithm, let us consider its suitable extension allowing us to address constraints of the form of Eq. (26). Our approach proceeds as follows:

1. if there are no constraint violations, solve the problem $\mathcal{Q}_I^{(k)}$ without (19).

2. if the attitude constraint (13) is not satisfied at the k_a-th step and the estimated sum $\tilde{s}(k_a, k_b)^\dagger$ is less than ϕ_1, proceed with Step 1. Otherwise, solve SDP $\mathcal{Q}_{II}^{(k)}$, below, repeatedly to escape the attitude exclusive zone:

$$\min_{x(k)} \quad \alpha + M\beta \tag{27}$$

subject to

$$x(k)^T \{H^T \tilde{A}_i H\} x(k) \le \beta, \quad i = 1, 2, \ldots, m,$$

†One way to estimate $s(k_a, k_b)$ is by directly integrating Eqs. (1)-(3) and (5) with a pseudo control force.

or equivalently the LMIs

$$\begin{bmatrix} \mu_i + \beta & (Hx(k))^T \\ Hx(k) & (\mu_i I_{10} + \tilde{A}_i)^{-1} \end{bmatrix} \geq 0, \quad i = 1, 2, \ldots, m \tag{28}$$

in conjunction with Eq. (20)-(23), with M chosen as a large positive constant.

A moment reflection on the inclusion of parameter M in the objective functional (27) reveals that this modified objective ensures that the algorithm guides the spacecraft attitude to leave the constrained region as quickly as possible. This on the other hand leads to an attitude maneuver that respects the integral constraint (25) that characterizes Type-II constraints.

III-C Type-III Constraints

We now consider Type-III constraints of the form

$$v(t)^T w(t) \leq \cos\theta, \tag{29}$$

where both vectors v and w are assumed to be controlled and time-varying. In view of the coordinate transformation in Eq. (12), we realize that Eq. (29) is no longer quadratic in the corresponding attitude quaternions q^v and q^w, where by (12) one has

$$\begin{aligned} v(t) &= v_B(t) - 2\,(q_o^v(t)^T q_o^v(t))\, v_B(t) + 2\,(q_o^v(t)^T v_B(t))\, q_o^v(t) \\ &+ 2q_4^v(t)\,(v_B(t) \times q_o^v(t)) \qquad (30) \\ w(t) &= w_B(t) - 2\,(q_o^w(t)^T q_o^w(t))\, w_B(t) + 2\,(q_o^w(t)^T w_B(t))\, q_o^w(t) \\ &+ 2q_4^w(t)\,(w_B(t) \times q_o^w(t)). \qquad (31) \end{aligned}$$

Nevertheless, we will shortly expand on few observations that make the SDP approach of §III-A still viable for this more complex scenario. First recall that attitude constraints of Type-III are of the form

$$\begin{bmatrix} v(t) \\ w(t) \end{bmatrix}^T \begin{bmatrix} 0_{3\times3} & I_3 \\ I_3 & 0_{3\times3} \end{bmatrix} \begin{bmatrix} v(t) \\ w(t) \end{bmatrix} \leq 2\,\cos\theta. \tag{32}$$

In the case where the quaternions are accurately updated, i.e., when both $q^v, q^w \in \mathbf{B}_1$ apriori, one has

$$\left\| \begin{bmatrix} v(t) \\ w(t) \end{bmatrix} \right\| = (\|v(t)\|^2 + \|w(t)\|^2)^{\frac{1}{2}} = \sqrt{2}.$$

Thus

$$[v(t)^T\, w(t)^T]^T \in \mathbf{B}_{\sqrt{2}},$$

and in view of Proposition III.1, Eq. (32) can be convexified as

$$\begin{bmatrix} 2\,(\mu+\cos\theta) & \begin{bmatrix} v(t) \\ w(t) \end{bmatrix}^T \\ \begin{bmatrix} v(t) \\ w(t) \end{bmatrix} & D \end{bmatrix} \geq 0, \tag{33}$$

where μ is chosen such that

$$D := (\mu\, I_6 + \begin{bmatrix} 0_{3\times 3} & I_3 \\ I_3 & 0_{3\times 3} \end{bmatrix})^{-1} \in \mathbf{S}^n_{++}. \tag{34}$$

Let us now consider the scenario where the quaternions are updated via a linearization scheme and thus†

$$\|\hat{q}(t)\| = \gamma \geq 1.$$

Recall that by (30) one has

$$v(t) = v_B(t) + u_B(t)$$

where

$$u_B(t) := -2\{q_o^v(t)^T q_o^v(t)\}\, v_B(t) + 2\,\{q_o^v(t)^T v_B(t)\}\, q_o^v(t) + 2q_4^v(t)\{v_B \times q_o^v(t)\}.$$

Note that when $q(t) \in \mathbf{B}_1$, $\|v(t)\| = \|v_B\| = 1$, and

$$\|v(t)\|^2 = \|v_B(t) + u_B(t)\|^2 = \|v_B(t)\|^2 + 2\, v_B(t)^T u_B(t) + \|u_B(t)\|^2,$$

or in other words,

$$2\, v_B(t)^T u_B(t) = -\|u_B(t)\|^2, \quad \text{for all } t. \tag{35}$$

Now returning to the case when it is only known that $\hat{q}(t) \in \widehat{\mathbf{B}}_1$, let

$$\hat{v}(t) := v_B(t) + \hat{u}_B(t),$$

†We will adopt the convention of putting " ^ " on quantities that are approximate due to the linearization scheme.

where

$$\hat{u}_B(t) := -2\{\hat{q}^v_o(t)^T\hat{q}^v_o(t)\}v_B(t) + 2\{\hat{q}^v_o(t)^T v_B(t)\}\hat{q}^v_o(t) + 2\hat{q}^v_4(t)\{v_B(t) \times \hat{q}^v_o(t)\},$$

i.e., for the specific time instance t, one has $\hat{u}_B(t) = \gamma^2 u_B(t)$ with $\gamma \geq 1$. Then,

$$\begin{aligned}\|\hat{v}(t)\|^2 &= \|v_B(t) + \hat{u}_B(t)\|^2 = \|v_B(t) + \gamma^2 u_B(t)\|^2 \\ &= \|v_B(t)\|^2 + 2\,\gamma^2 v_B(t)^T u_B(t) + \gamma^4 \|u_B(t)\|^2 \\ &= \|v_B(t)\|^2 + (\gamma^4 - \gamma^2)\;\|u_B(t)\|^2;\end{aligned}$$

in view of Eq. (35), we conclude that

$$\|\hat{v}(t)\|^2 \geq \|v_B\|^2$$

which implies that

$$\|\begin{bmatrix} \hat{v}(t) \\ \hat{w}(t) \end{bmatrix}\| \geq \|\begin{bmatrix} v(t) \\ w(t) \end{bmatrix}\| = \sqrt{2}.$$

Thereby, even in the case where a linearization scheme is utilized for quaternions updates, one has $[\hat{v}(t)\;\hat{w}(t)] \in \widehat{\mathbf{B}}_{\sqrt{2}}$; thus Proposition III.2 can be invoked to derive a sufficient LMI condition enforcing the inequality (29). Furthermore, in order to include (30)-(31) in our optimization framework, representing the relation between vectors represented in inertial and body coordinate frames, we add an additional six quadratic inequalities to our SDP formulation. As an example, for the first coordinate of $v(t)$, $v_1(t)$, one can write

$$q^v(t)^T C^v_1 q^v(t) = v_1(t) - (v_B)_1(t),$$

where

$$C^v_1 = \begin{bmatrix} 0 & (v_B)_2 & (v_B)_3 & 0 \\ (v_B)_2 & -2\,(v_B)_1 & 0 & -(v_B)_3 \\ (v_B)_3 & 0 & -2\,(v_B)_1 & (v_B)_2 \\ 0 & -(v_B)_3 & (v_B)_2 & 0 \end{bmatrix}$$

and $v_B = [(v_B)_1, (v_B)_2, (v_B)_3]^T$, that can be represented by quadratic inequalities,

$$q^v(t)^T C^v_1 q^v(t) \geq v_1(t) - (v_B)_1, \tag{36}$$

and

$$q^v(t)^T C^v_1 q^v(t) \leq v_1(t) - (v_1)_B. \tag{37}$$

Now Proposition III.1 can be applied to (36)-(37) in order to convexify these inequalities by representing them as

$$L^v_{1+}(t) := \begin{bmatrix} \mu_1 - v_1(t) + (v_1)_B & q^v(t)^T \\ q^v(t) & (\mu_1 I_4 - C^v_1)^{-1} \end{bmatrix} \geq 0$$

and

$$L^v_{1-}(t) := \begin{bmatrix} \mu_2 + v_1(t) - (v_1)_B & q^v(t)^T \\ q^v(t) & (\mu_2 I_4 + C^v_1)^{-1} \end{bmatrix} \geq 0,$$

where μ_1 and μ_2 are strictly greater than the largest eigenvalues of C^v_1 and $-C^v_1$ in (36)-(37), respectively. Thus, our SDP formulation of the constrained attitude control with Type-III constraints, involves iterations $Q^{(k)}_{III}$ of the form

$$\min_{x^v(k),\, x^w(k),\, v(k+2),\, w(k+2)} \quad \alpha^v + \alpha^w$$

subject to

$$\begin{bmatrix} 2\,(\mu + \cos\theta) & \begin{bmatrix} v(k+2) \\ w(k+2) \end{bmatrix}^T \\ \begin{bmatrix} v(k+2) \\ w(k+2) \end{bmatrix} & D \end{bmatrix} \geq 0,$$

$$L^v_{j+}(k+2) \geq 0, \quad L^v_{j-}(k+2) \geq 0, \quad L^w_{j+}(k+2) \geq 0, \quad L^w_{j-}(k+2) \geq 0,$$

where D is defined by Eq. (34) and $j \in \{1, 2, 3\}$, in conjunction with constraints (20)-(23) associated with variables $x^v(k)$ and $x^w(k)$.

III-D Type-IV Constraints

The most remarkable feature of the SDP approach is its ability to handle various combinations of all foregoing types of constraints while maintaining the guaranteed convergence property. In this venue, we notice that all these constraints can accurately be represented by LMIs. Such a representation, on the other hand, leads to a semidefinite programming solution to a wide array of CAC problems augmented with mixed constraints. Table 1 summarizes the applicability and convergence properties of the various algorithmic frameworks for solving the CAC problem as considered in this paper.

approach	Type-I	Type-II	Type-III	Type-IV	convergence
geometric	$\surd$	–	–	–	$\surd$
potential function	$\surd$	–	–	–	–
constraint monitoring	$\surd$	$\surd$	$\surd$	$\surd$	–
randomized	$\surd$	$\surd$	$\surd$	$\surd$	–
SDP	$\surd$	$\surd$	$\surd$	$\surd$	$\surd$

Table 1: Applicability and convergence properties of the various frameworks for solving the CAC problem.

IV Simulation Results

In this section, we present an example for solving a CAC problem subject to a Type-III constraint via the SDP approach of §III. As mentioned in §II-A, multiple spacecraft formation flying missions are of the main source of this class of problems. Specifically, we consider the problem of constrained relative attitude control in a dual-spacecraft mission. The two spacecraft, denoted by SC_1 and SC_2, have thrusters capable of providing control torques aligned with each principal axes; SC_1 is assumed to have an on-board sensitive instrument. Our objective is to find a sequence of control torques $u(k)$ $(k = 0, 1, 2, \ldots)$, such that SC_1 and SC_2 change their orientations from initial states $(q_1(t_0), \omega_1(t_0))$ and $(q_2(t_0), \omega_2(t_0))$, to final states $(q_1(t_f), \omega_1(t_f))$ and $(q_2(t_f), \omega_2(t_f))$, while the sensitive instrument on-board SC_1 is not in a constrained cone around particular thrust directions emanating from SC_2 during the entire attitude slew. The physical constants and the initial and terminal conditions for our example are as follows: spacecraft masses are 1 kg, principle axes of inertia are

$$\textbf{Diag}\,[J_1, J_2, J_3] = \textbf{Diag}\,[100, 200, 300]\ \text{kg m}^2,$$

initial angular velocities,

$$\omega_1(t_0) = \omega_2(t_0) = [0, 0, 0]^T\ \text{rad/sec},$$

final angular velocities,

$$\omega_1(t_f) = \omega_2(t_f) = [0, 0, 0]^T\ \text{rad/sec},$$

initial attitude quaternions,

$$\begin{aligned} q_1(t_0) &= [0.0000, 0.0000, 0.0000, 1.0000]^T, \\ q_2(t_0) &= [-0.5000, 0.5000, 0.5000, 0.5000]^T, \end{aligned}$$

final attitude quaternions,

$$\begin{aligned} q_1(t_f) &= [-0.5000, 0.5000, 0.5000, 0.5000]^T, \\ q_2(t_f) &= [0.0000, 0.0000, 0.0000, 1.0000]^T, \end{aligned}$$

the sensitive instrument vector in the body frame attached to SC_1 is,

$$v_B = [0.750, 0.433, 0.500]^T,$$

the thruster vectors in the body coordinate frame attached to SC_2 are,

$$(w_1)_B = [1, 0, 0]^T, \quad (w_2)_B = [0, 1, 0]^T, \quad (w_3)_B = [0, 0, 1]^T,$$

and finally, the required angular separation is required to be $\theta = 50$ deg. The initial and the desired final attitude quaternions have been chosen to satisfy (29), i.e., the sensitive instrument on SC_1 is outside the three constraint cones emanating from the bore-sight of each thruster on SC_2, or more precisely,

$$\begin{aligned} v(t_0)^T w_1(t_0) &\leq \cos\theta \; (= 0.6428), \\ v(t_0)^T w_2(t_0) &\leq \cos\theta, \\ v(t_0)^T w_3(t_0) &\leq \cos\theta, \end{aligned}$$

where v and w_1, w_2, w_3 are the inertially represented vectors corresponding to u_B and $(w_1)_B$, $(w_2)_B$, $(w_3)_B$, respectively. Figure 2 depicts the geodesic distance to the final attitudes for SC_1 (solid line) and SC_2 (dotted line) under the guidance of the SDP-based reconfiguration algorithm. In Figure 3, each line represents the value of $v(t)^T w_i(t)$ for $i = 1$ (solid line), 2 (dotted line), and 3 (dashed line). As seen in this figure, the constraints $v(t)^T w_2(t) \leq \cos\theta$ and $v(t)^T w_1(t) \leq \cos\theta$ successively become active at 5.1 sec and 29.8 sec, and the corresponding values of $v(t)^T w_i(t)$ $(i = 2, 1)$ stay constant at $\cos\theta = 0.6428$ until 699.3 sec and 810.8 sec, respectively. One interesting observation is that the value of $v(t)^T w_3(t)$, where $t \in [29.8\,\text{sec}, 699.3\,\text{sec}]$, remains constant even when the corresponding constraint does not explicitly become active during the maneuver. Figure 4 depicts the control torques about the x-axis exerted on SC_1 (solid line) and SC_2 (dotted line). This figure also shows that once one of the constraints becomes active, two negative control torques are automatically generated. In our example, as a remedy for the numerical issues that were pointed out in §III-C, pertaining to quaternion updates at each time step, Eq. (24) has been embedded in the proposed SPD-based framework.

V Concluding Remarks

In this paper, we first provided a survey of existing methods for solving the constrained attitude control problem as it arises in a wide range of space science missions. The viability of these approaches was then considered in the context of several types of attitude constraints. Subsequently, the SDP-based approach was shown to provide a unifying venue through which various classes of attitude constraints can be addressed via an elegant, efficiently solvable optimization framework.

Acknowledgments

The research of Y. Kim and M. Mesbahi was supported by NSF grant CMS-0093456 and by a grant from Jet Propulsion Laboratory, California Institute of Technology, under a contract with the National Aeronautics and Space Administration. The research of G. Singh and F. Y. Hadaegh was carried out at the Jet Propulsion Laboratory, California Institute of Technology, under a contract with the National Aeronautics and Space Administration.

References

[1] Ahmed, A., Alexander, J., Boussalis, D., Breckenridge, W., Macala, G., Mesbahi, M., San Martin, M., Singh, G., and Wong, E., "Cassini Control Analysis Book," Jet Propulsion Laboratory, 1998.

[2] Collaudim, B., and Passvogel, Th., "The FIRST and Planck Carrior Missions: Description of Cryogenic Systems," Space Cryogenics Workshop, ESA Paper WPP-157, 1999, pp. 111–122.

[3] Frakes, J. P., Henretty, D. A., Flatley, T. W., Markley, F. L., San, J. K., and Lightsey, E. G., "SAMPEX Science Pointing with Velocity Avoidance," *AAS/AIAA Spaceflight Mechanics Meeting*, AAS Paper 92-182, 1992, pp. 949-966.

[4] Wen, J., and Kreutz-Delgado, K., "The Attitude Control Problem," *IEEE Transactions on Automatic Control*, Vol. 36, No. 10, 1991, pp. 1148–1161.

[5] Kim, Y., and Mesbahi, M., "Quadratically Constrained Spacecraft Attitude Constrained Control Via Semidefinite Programming," *IEEE Transactions on Automatic Control*, Vol. 49, No. 5, 2004, pp. 731-735.

[6] Hablani, H. B., "Attitude Commands Avoiding Bright Objects and Maintainig Communication with Ground Station," *Journal of Guidance, Control, and Dynamics*, Vol. 22, No. 6, 1999, pp. 759-767.

[7] Spindler, K., "New Methods in On-board Attitude Control," Advanced in the Astronautical Sciences, Vol. 100, No. 2, 1998, pp. 111-124.

[8] McInnes, C. R., "Large Angle Slew Maneuvers with Autonomous Sun Vector Avoidance," *Journal of Guidance, Control, and Dynamics*, Vol. 17, No. 4, 1994, pp. 875-877.

[9] Wisniewski, R., "Slew Maneuver Control for Spacecraft Equipped with Star Camera and Reaction Wheels," Control Engineering Practice, 2004, to appear.

[10] Singh, G., Macala, G., Wong, E., and Rasmussen, R., "A Constraint Monitor Algorithm For The Cassini Spacecraft," *Proceedings of the AIAA Guidance, Navigation, and Control Conference*, AIAA, Reston, VA, 1997, pp. 272-282.

[11] Frazzoli, E., Dahleh, M. A., Feron, E., and Kornfeld, R., "A randomized attitude slew planning algorithm for autonomous spacecraft," *Proceedings of the AIAA Guidance, Navigation, and Control Conference*, AIAA, Montreal, Canada, 2001.

[12] Cheng, P., Frazzoli, E., and LaValle, S., "Improving the Performance of Sampling-Based Planners by Using a Symmetry-Exploiting Gap Reduction Algorithm," *Proceedings of the IEEE International Conference on Robotics and Automation*, New Orleans, CA, 2004, pp. 4362-4368.

[13] Sorensen, A. M., "ISO Attitude Maneuver Strategies," American Astronautical Society, AAS Paper 93-317, 1993, pp. 975-987.

[14] Boyd, S. P., El Ghaoui, L., Feron, E., and Balakrishnan, V., *Linear Matrix Inequalities in System and Control Theory*, Society for Industrial and Applied Mathematics, Philadelphia, 1994.

[15] *http://fewcal.kub.nl/sturm/software/sedumi.html*.

[16] Kuipers, J. B., *Quaternions and Rotation Sequences*, Princeton University Press, Princeton, New Jersey, 1999.

List of Figures

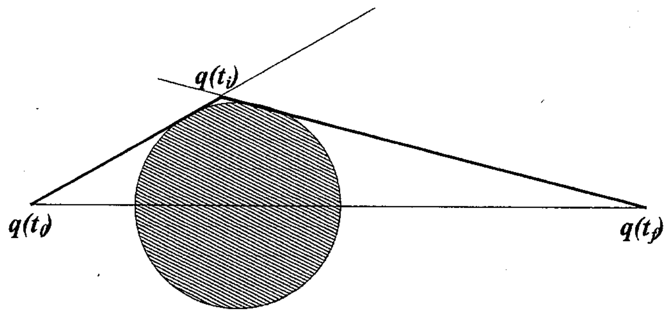

Figure 1: A tangential exclusion path $q(t_0) \rightsquigarrow q(t_i) \rightsquigarrow q(t_f)$ around the Sun (shaded area)

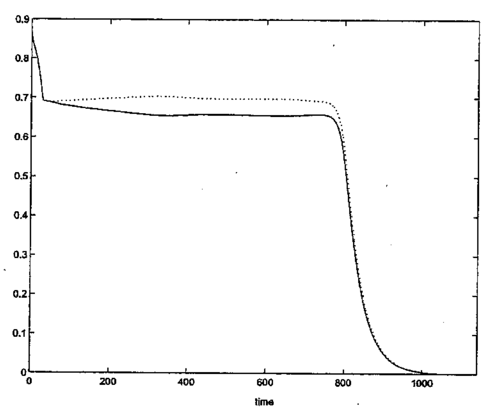

Figure 2: Geodesic deviation between current and final attitudes for SC_1 (solid line) and SC_2 (dotted line).

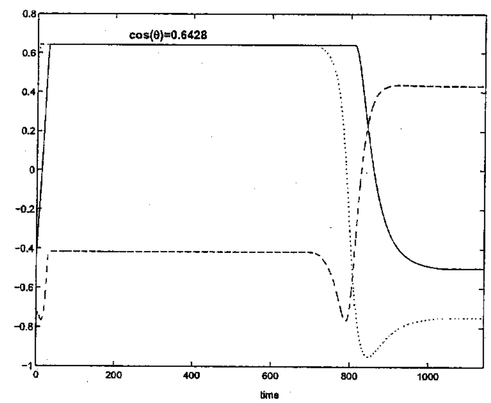

Figure 3: The inner products between inertially represented sensitive instrument vector $v(t)$ and thruster vectors $w_i(t)$ $(i = 1, 2, 3)$: $v(t)^T w_1(t)$ (solid line), $v(t)^T w_2(t)$ (dotted line), and $v(t)^T w_3(t)$ (dashed line).

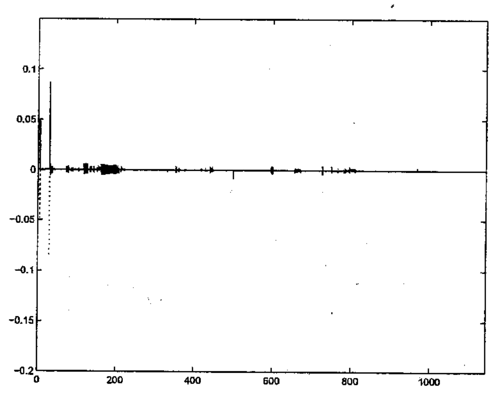

Figure 4: Control torques about the x-axis exerted on SC_1 (solid line) and SC_2 (dotted line).